

Anisotropic hysteresis on ratcheted superhydrophobic surfaces

H. Kusumaatmaja^{a,b} and J. M. Yeomans^a

^aThe Rudolf Peierls Centre for Theoretical Physics, Oxford University, 1 Keble Road, Oxford OX1 3NP, U.K. and

^bMax Planck Institute of Colloids and Interfaces, Science Park Golm, 14424 Potsdam, Germany

(Dated: November 21, 2018)

We consider the equilibrium behaviour and dynamics of liquid drops on a superhydrophobic surface patterned with sawtooth ridges or posts. Due to the anisotropic geometry of the surface patterning, the contact line can preferentially depin from one side of the ratchets, leading to a novel, partially suspended, superhydrophobic state. In both this configuration, and the collapsed state, the drops show strong directional contact angle hysteresis as they are pushed across the surface. The easy direction is, however, different for the two states. This observation allows us to interpret recent experiments describing the motion of water drops on butterfly wings.

Superhydrophobic surfaces [1] show extreme water repellency, with effective contact angles that can be close to 180° . Superhydrophobicity results when the natural hydrophobicity of a substrate is amplified by roughness. Typically a drop on a superhydrophobic surface can either lie in a Cassie-Baxter state [2], suspended on top of the roughness with air-pockets beneath, or in the Wenzel state [3], where the liquid penetrates the spaces between the surface corrugations. The drop contact angle is enhanced in both the Wenzel and the Cassie-Baxter states but the dynamical behaviour of the two configurations is very different; a liquid drop in the suspended state is highly mobile, while that in the collapsed state is strongly pinned.

Superhydrophobic surfaces have evolved naturally in many contexts. Plants, such as the lotus, nasturtium and Lady's Mantle have superhydrophobic leaves to aid the run-off of rain [4]. The plasteron used by aquatic insects to breathe underwater is air trapped beneath a Cassie-Baxter interface, and hairs on the legs of water insects render them superhydrophobic and lead to enhanced buoyancy [5]. In a recent paper Zheng *et al.* [6] reported that butterfly wings are hydrophobic and that they are patterned by an arrangement of anisotropic scales of typical size $100\mu m$. These authors found that liquid drops placed on the wings roll easily away from the insect's body, but are pinned strongly against movement in the opposite direction, towards the body.

Motivated by this work we investigate the behaviour of drops on a hydrophobic surface patterned with ratchets, posts which have sides of different slopes, see Fig. 1. We identify a novel, partially suspended, superhydrophobic state and describe its regions of stability. We then simulate the hydrodynamics of drops pushed across the ratchets. We find that the partially suspended and collapsed configurations both have a highly anisotropic response to a driving force, effectively functioning as 'fluidic diodes'. Surprisingly, the easy direction is opposite for the two configurations, primarily due to the behaviour of the receding contact line. The new results enable us to explain the motion of raindrops on butterfly wings.

Consider a large liquid drop lying on a regular array of hydrophobic ridges, one side of which makes an angle α with the horizontal, and the other side of which is vertical, as shown in Fig. 1. Figs. 1(a) and (b) depict the Cassie-Baxter, or suspended, and Wenzel, or collapsed, configurations respectively. On a ratcheted surface, however, a third configuration is possible. We shall term this, shown in Fig. 1(c), the partially suspended state.

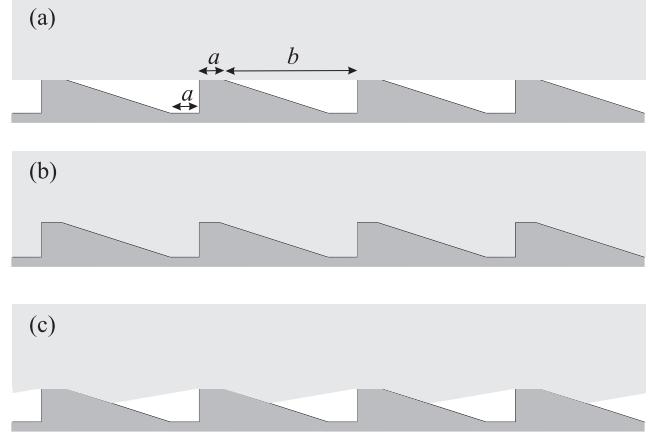


FIG. 1: Schematic diagram of a drop on a hydrophobic surface patterned with ratchets. (a) Suspended, (b) collapsed and (c) partially suspended state.

The partially suspended state is stable because, when a drop is placed gently onto a ratcheted surface, the Gibb's criterion [7] states that the interface will remain pinned at the ridge corners if the angle between the interface and the sides of the ratchets is less than the intrinsic equilibrium contact angle of the flat surface θ_e [8, 9]. For strongly superhydrophobic surfaces and large values of α this criterion is satisfied and the drop remains in the Cassie-Baxter state. As the wettability of the surface is increased, or α is decreased, depinning will occur. This happens first on the corner abutting the ridge side with the smallest gradient. For a drop, large compared to the size of the ridges, but small enough that gravity can be neglected, the condition for depinning is (for the two-dimensional, ridged geometry)

$$\theta_e < \pi - \alpha. \quad (1)$$

The transition is reversible: the contact line moves slowly down the sloping side of the ratchets as θ_e is decreased from the threshold value, and the interface will move back to the corner if the contact angle is increased above the value given in Eq. (1).

As the equilibrium contact angle or α is decreased further the drop depins from the second corner and moves down the vertical side of the ridges thus collapsing to the Wenzel state.

For a large drop this happens when

$$\theta_e = \frac{3\pi}{4} - \frac{\alpha}{2}. \quad (2)$$

Once depinning has occurred the interface moves immediately to the base of the grooves. This transition is irreversible, because the liquid–gas and gas–solid interfaces are replaced by a single liquid–solid interface, and there is an energy barrier to re-forming the gas layer.

The regions of stability of the different states, for an infinite drop initially placed on top of the ratchets, are summarised in Fig. 2(a). For $a = 0$, the figure also represents the phase diagram, ie the global minimum of the free energy.

Cassie-Baxter and Wenzel used simple thermodynamic arguments to derive the effective macroscopic (observable) contact angle for drops on superhydrophobic surfaces. Their formulae are applicable for drops covering a large number of ridges, which are not pinned with respect to motion across the surface. For the geometry we consider, arguments of this sort give a macroscopic contact angle

$$(a + b) \cos(\theta_{C-B}) = a \cos(\theta_e) - b, \quad (3)$$

$$(a + b) \cos(\theta_{PS}) = a \cos(\theta_e) + b \cos(\theta_e + \alpha), \quad (4)$$

$$(a + b) \cos(\theta_W) = \left(2a + \frac{(b - a)(1 + \sin \alpha)}{\cos \alpha} \right) \cos(\theta_e) \quad (5)$$

for the Cassie-Baxter, partially suspended, and Wenzel state respectively. Fig. 2(b) compares the macroscopic angles of the three states as a function of α for $\theta = 5\pi/8$ and $a/b = 0.1$. The state with the lowest contact angle corresponds to the minimum energy configuration [10, 11].

We now discuss finite drops and the way in which changes in drop radius of curvature, due to, say, evaporation or application of external pressure, can lead to transitions. For finite drop radius the curvature of the drop makes it easier for it to depin from the corners of the ratchets and the transition from the suspended to partially suspended state occurs at

$$Rc_1 = \frac{b}{2 \sin(\theta_e + \alpha - \pi)}. \quad (6)$$

Indeed for sufficiently small α , θ_e and R the suspended state is never stable, and the drop falls immediately into the partially suspended state. As the drop size is decreased further depinning from the second corner of the ratchet occurs at

$$Rc_2 = \frac{b \tan(\alpha) \sin(\pi/4 - \alpha/2)}{\sin(\theta_e + \alpha/2 - 3\pi/4)}. \quad (7)$$

These boundaries are shown in Fig. 2(c) as a function of θ_e and α for $R/b = 0.25$ and in Fig. 2(d) as a function of θ_e and b/R for $\alpha = \pi/4$.

For an infinite drop the depinned interface moves immediately to the bottom of the groove. However this is no longer the case for a finite drop. Because of the “V” shape geometry,

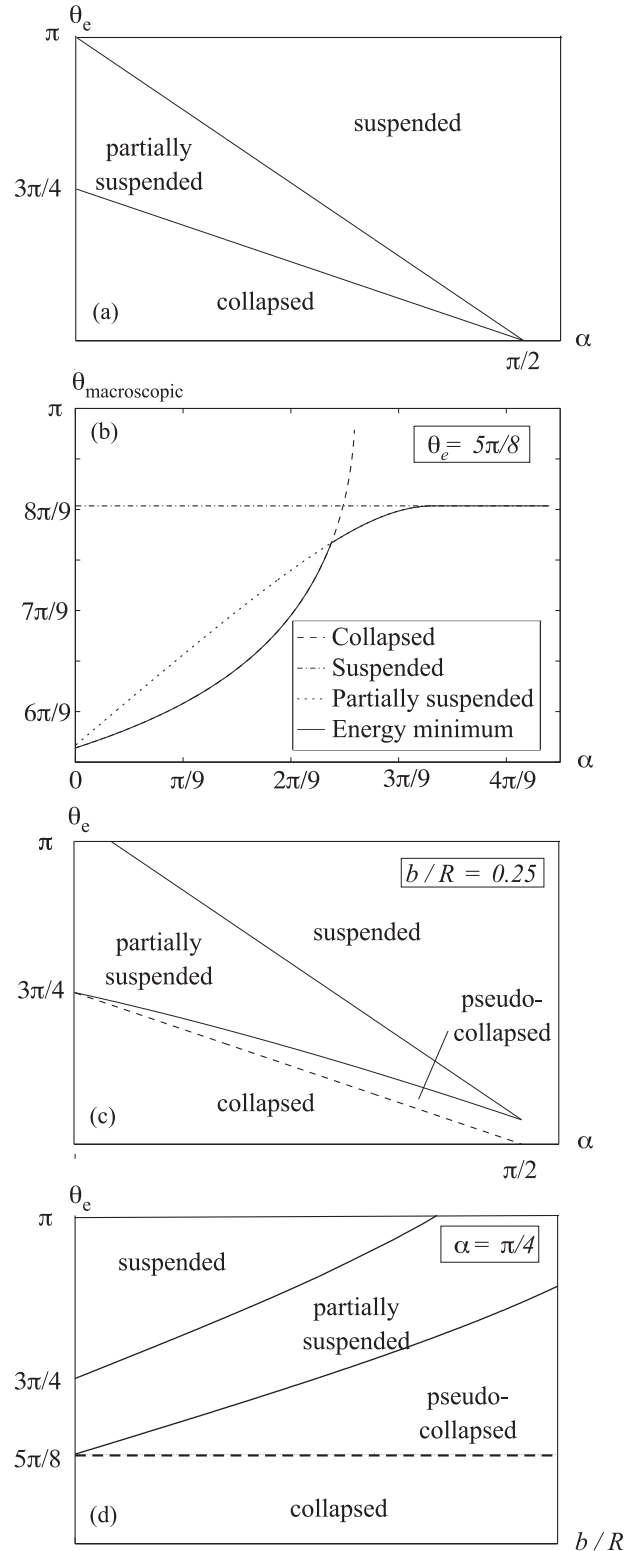


FIG. 2: (a) Regions of stability of the suspended, partially suspended and collapsed states of an infinite drop placed gently on a two-dimensional ratcheted surface. (b) Variation of the macroscopic contact angle with the ratchet angle α for $\theta_e = 5\pi/8$ and $a/b = 0.1$. (c) as (a), but for a finite drop, $b/R = 0.25$, (d) Regions of stability of the different states, for varying contact angle and drop size, for $\alpha = \pi/4$.

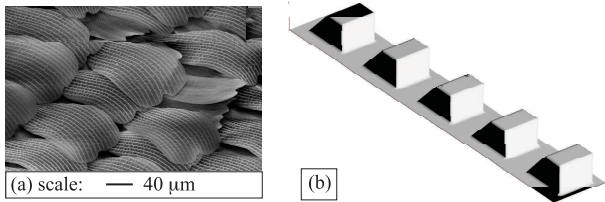


FIG. 3: (a) The wings of *Papilio palinurus*. The figure is kindly provided by Prof. S. Berthier. (b) The surface patterning used to obtain Fig. 4.

the pressure set up by the sides of the grooves (because the local contact angle is equal to the Young's angle in equilibrium) increases as the drop penetrates them. This means that the interface moves slowly down the ridges as the drop volume decreases: there is a stable interface profile for a given drop volume, or equivalently, for a given external pressure [12]. We shall term this the 'pseudo-collapsed' state as its dynamical properties are similar to those of a Wenzel configuration. The transition from partially suspended to pseudo-collapsed is reversible, the contact line moves slowly up and down the sides of the ratchets as a function of the Laplace pressure. The drop remains in the pseudo-collapsed configuration until the condition given in Eq. (2) is satisfied, at which point the interface slides immediately to the bottom of the groove. This transition is irreversible. Fig. 2(c) shows the configurations which are global minima of the free energy for $a = 0$ and $b/R = 0.25$. For $a \neq 0$ the sequence of transitions is truncated by a discontinuous change to the Wenzel configuration immediately the interface touches the base of the grooves.

For a drop on posts, rather than ridges, it is not possible to describe the transitions analytically, because of the two-dimensional curvature of the interfaces between the posts. However the same quantitative behaviour is expected. Indeed, a sequence of depinning transitions could occur on posts with facets of different slopes.

We now compare the dynamics of drops in the suspended, partially suspended and collapsed configurations, considering a cylindrical liquid drop confined between surfaces patterned with posts. This geometry was chosen because it includes the important physics of the three dimensional problem, namely the two dimensional curvature of the interface between the posts, while being less demanding of computational resources than modelling a full three dimensional drop. (A more restricted set of simulations of drops sitting on top of a single ratcheted surface gave qualitatively the same behaviour.) Guided by the patterning on the wings of *Papilio palinurus*, shown in Fig. 3(a), the posts were taken to have three vertical and one sloping side (see Fig. 3(b)). On butterfly wings, the sloping angle α is typically of order 10° but here, to restrict the inter-ridge spacing to a computationally feasible value, we have used $\alpha = 45^\circ$.

The drop thermodynamics was described by a binary free energy model and the hydrodynamics by the corresponding Navier-Stokes equations, solved using a lattice Boltzmann algorithm. This approach is proving a useful tool to study drop

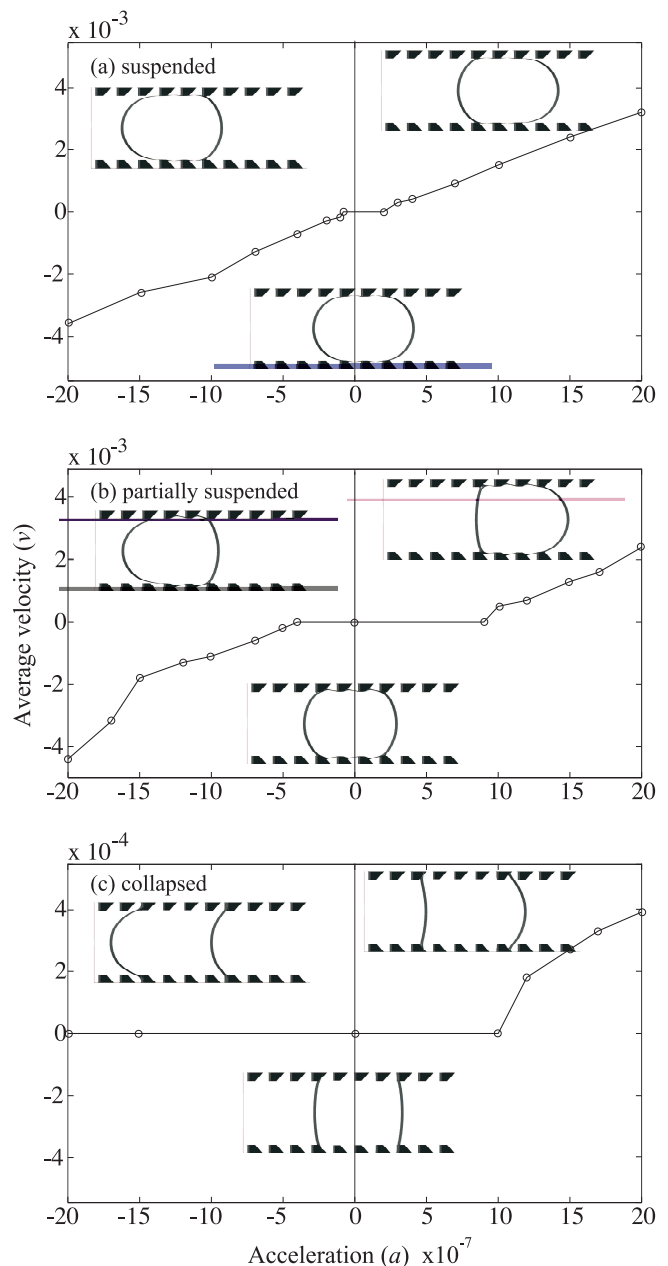


FIG. 4: Comparison of the mean velocity of (a) suspended ($\theta_e = 140^\circ$), (b) partially suspended ($\theta_e = 110^\circ$) and (c) collapsed ($\theta_e = 100^\circ$) drops as a function of the applied acceleration. Drop shapes in equilibrium and when moving in different directions are shown in the insets. The other parameters of the simulations are: surface tension $\gamma = 0.013$, liquid drop viscosity $\eta_{\text{liquid}} = 0.83$, surrounding gas viscosity $\eta_{\text{gas}} = 0.06$. All data is in simulation units.

motion in situations where pinning and hysteretic effects are important. Details of the model and algorithm can be found in [13, 14] and the references therein.

Fig. 4 compares the motion of a drop in the suspended, partially suspended and collapsed states. The intrinsic contact angles for the three states are $\theta_e = 140^\circ$, 110° and 100° respectively and the drop covered ~ 4 posts. The drop was pushed by a variable body force parallel to the surface; we choose to

refer to the direction from the vertical to the sloping edge of the posts as positive (to the right in Fig. 4).

The average velocity as a function of the applied force is shown in Fig 4. There is a striking difference between the three configurations. In the suspended state the pinning is weak, and essentially independent of direction. In the collapsed state, however, there is strongly anisotropic pinning and the drop does not move at all in the negative direction for forces in the range we have considered. This occurs because the interface is strongly pinned with respect to movement down the vertical sides of the posts [15]. Once the drop is moving, the velocity for a given force is a factor ~ 10 lower in the collapsed than in the suspended state.

A pronounced asymmetry in the pinning threshold is also seen for the partially suspended state, but note that the negative direction is now the *easy* direction. This surprising behaviour is a result of the shape of the liquid–gas interface underneath the drop. From the simulations, we find that the motion of the drop is primarily controlled by pinning at the receding contact line. For a partially suspended drop pushed in the positive direction, the receding interface lies part-way down the posts and the drop dynamics are those of a collapsed state, with strong pinning. If the drop is pushed in the negative direction, however, the trailing edge lies on top of the posts and the drop behaves like a suspended state, with low contact angle hysteresis [16].

Butterfly wings form a ratcheted surface, albeit a much more structured one than that we consider here. The wings are covered with overlapping scales of length $\sim 100\mu\text{m}$, with free ends pointing towards the wing tips (Fig. 3(a)). Drops of water are observed to run away from the butterfly body: Zheng *et al.* [6] reported that on the wings of *Morpho aega*, the pinning threshold is > 6 times stronger for motion towards the body.

The easy direction for the butterfly corresponds to the negative direction in our simulation geometry, and hence the easy direction for the partially suspended state, which should be

stabilised by the anisotropic wing patterning. We do, however, find a less strong anisotropy in the simulations, and it will be interesting to investigate which model parameters are key in controlling this. We note that a secondary structure of ridges of height $\sim 0.5\mu\text{m}$ running along each scale are observed on the butterfly wings. This is not needed to contribute to the anisotropic hysteresis, but could be useful in preventing lateral run-off or in increasing the effective contact angle of the surface [17].

Anisotropic surface patterning is not limited to butterfly wings. For example, several authors (*e.g.* [5]) have shown that the legs of insects such as water striders are covered with hairs that are tilted by $\sim 60^\circ$ from the vertical direction. A possible role of the asymmetry is to introduce directionality to the motion of the insects on water surfaces.

We have considered a superhydrophobic surface patterned with sawtooth posts and shown that a partially suspended configuration can be stable in addition to the two usual, suspended and collapsed, phases. It is now feasible to construct ratcheted surfaces on micron length scales, so we hope that this letter will motivate experimental work identifying the novel configuration on both fabricated and biological surfaces.

Drops in both the partially suspended and collapsed states have an anisotropic response when they are pushed across the surface, but the easy direction is different in the two configurations. Furthermore, the transition between the partially suspended and the pseudo-collapsed state can be induced reversibly by the changing the drop pressure or contact angle (which can be done via electrowetting). This opens up the possibility of constructing a ‘fluidic diode’, with external control of the easy direction, for use in microfluidic devices.

We thank S. Brewer, M. Blow, K. Hermans, R. Lipowsky, and R. Vrancken for useful discussions. We gratefully acknowledge Prof. S. Berthier (Institut des Nano-Sciences de Paris) for providing Fig. 3(a) and Prof. P. Vukusic (University of Exeter) for providing the picture of *Papilio palinurus* in our table of contents graphics entry.

-
- [1] D. Quéré, *Annu. Rev. Mater. Res.*, 2008, **38**, 71.
 [2] A. B. D. Cassie and S. Baxter, *Trans. Faraday Soc.*, 1944, **40**, 546.
 [3] R. N. Wenzel, *Ind. Eng. Chem.*, 1936, **28**, 988.
 [4] W. Barthlott and C. Neinhuis, *Planta*, 1997, **202**, 1.
 [5] J. W. M. Bush, D. L. Hu and M. Prakash, *Adv. Insect Physio.*, 2007, **34**, 117.
 [6] Y. M. Zheng, X. F. Gao, and L. Jiang, *Soft Matter*, 2007, **3**, 178.
 [7] J. W. Gibbs, *Scientific Papers 1906*, Dover (Dover reprint), New York, 1961.
 [8] H. Kusumaatmaja, M. L. Blow, A. Dupuis, and J. M. Yeomans, *Europhys. Lett.*, 2008, **81**, 36003.
 [9] A. Tuteja, W. Choi, M. Ma, J. M. Mabry, S. A. Mazzella, G. C. Rutledge, G. H. McKinley, R. E. Cohen, *Science*, 2007, **318**, 1618.
 [10] C. Ishino, K. Okumura, and D. Quéré, *Europhys. Lett.*, 2004, **68**, 419.
 [11] N. A. Patankar, *Langmuir*, 2004, **20**, 7097.
 [12] M. Brinkmann and R. Blossey, *Eur. Phys. J. E*, 2004, **14**, 79.
 [13] C. M. Pooley, H. Kusumaatmaja and J. M. Yeomans, *Phys. Rev. E*, 2008, **78**, 056709.
 [14] H. Kusumaatmaja, DPhil Thesis, University of Oxford, 2008.
 [15] A. Buguin, L. Talini and P. Silberzan, *Appl. Phys. A*, 2002, **75**, 207.
 [16] H. Kusumaatmaja and J. M. Yeomans, *Langmuir*, 2007, **23**, 6019.
 [17] L. Gao and T. J. McCarthy, *Langmuir*, 2006, **22**, 2966.